Hindawi
Advances in Civil Engineering
Volume 2022, Article ID 8785030, 11 pages
https://doi.org/10.1155/2022/8785030

Research Article

Disaster Risk Evaluation of Superlong Highways Tunnel Based on the Cloud and AHP Model

Zhi Li,[1,2] Xianqing Meng,[1] Dunwen Liu,[1] Yu Tang,[1] and Tan Chen[2]

[1]*School of Resources and Safety Engineering, Central South University, Changsha 410083, China*
[2]*Road & Bridge South China Engineering Co., LTD., Zhongshan 528403, China*

Correspondence should be addressed to Yu Tang; tangyu12@csu.edu.cn

Received 5 May 2022; Revised 29 May 2022; Accepted 30 May 2022; Published 13 June 2022

Academic Editor: Wen-Da Wang

Comprehensive evaluation of the geological disaster risk of super long tunnels is significant for safety construction. In this paper, we establish a comprehensive evaluation system based on the cloud model and analytic hierarchy process (AHP) theory, considering four kinds of geological hazards, such as water and mud inrush, large deformation, rock burst, and collapse. Then, based on a super long highway tunnel of the Chizhou-Qimen expressway in China, the construction risk evaluation is carried out. The results show that the evaluation system can accurately judge the disaster risk level of the tunnel under different conditions surrounding a rock. The cloud model theory can realize the mutual transformation of qualitative indicators and quantitative indicators and avoid the problem of intense subjectivity of evaluation indicators. The evaluation system can be used as a new approach to evaluate tunnel risks in similar projects.

1. Introduction

With the development of Chinese highway construction to mountainous areas, to meet the transport line requirements, the number of deep-buried and superlong tunnels is increasing. For example, the completed Jinping Mountain road tunnel in China has a maximum burial depth of 2,375 m. Compared to mountain roads, the deep-buried tunnel has the advantages of safer driving, shorter driving miles, savings in time and energy, and protection of the ecological environment of the surface. It has greatly promoted China's transportation construction, but on the contrary, it also brought new challenges for underground engineering technology. Due to its large burial depth and the number of different geological units traversed, in addition to the engineering geological problems of general tunnels, there are also a series of special or more serious problems than general tunnels [1]. For example, the Zhegushan Tunnel on the Sichuan-Tibet Highway caused collapse, initial support encroachment limit, and severe damage to the support structure due to large deformations of the surrounding rock. This caused a direct economic loss of approximately 20 million yuan and severely restricted the construction progress. Therefore, carrying out geological hazard risk evaluation of deep-buried tunnels is very important for the safe construction and operation of tunnel engineering.

Scholars from various countries have carried out a large number of studies on the hazard evaluation of tunnels. Among them, Q. Wang [2] proposed a method for evaluating rock burst grades of deep-buried and superlong tunnels based on a geographic information system (GIS) framework. The combination of GIS spatial data analysis methods provided a new method for predicting rock bursts. On the basis of the existing analysis theory of surrounding rock stability, R. Song [3] established a catastrophe model of the instability tip point of the surrounding rock of a deep-buried tunnel crossing the fault fracture zone, which provided new ideas for the risk evaluation of destabilization damage of surrounding rocks at the fault of the deep-buried tunnel. X. Jia [4] conducted an inverse analysis of the crustal stress characteristics of deep-buried superlong tunnels. Combined with comprehensive geological analysis and the extension method

to summarize, he analyzed and predicted the basic law of large deformation and rock burst in the Erlangshan tunnel. Based on the hierarchical analysis method, Z. Xu [5] calculated the weight values of the main control factors of water and mud inrush of the karst tunnel and proposed a 3-stage evaluation method for the risk of water and mud inrush in karst tunnels, which was successfully applied in engineering practice. B. Wu [6] analyzed more than 100 mountain tunnel collapse cases in China and organically combined the respective advantages of the expert scoring method, the comprehensive fuzzy evaluation method, and the network analysis method to build a tunnel construction collapse risk evaluation model for the drilling-blasting method. However, the existing research does not consider the changes in the risk of disasters in different sections of the tunnel. Generally, only one type of disaster and a typical road section are selected for risk evaluation. While in tunnel construction, deep-buried and superlong tunnels often have different disaster risks in different sections due to the large burial depths, long distances, complex terrain crossing, and variable geological conditions. In addition, there are ambiguities and randomness among various factors in complex evaluation systems [7], and existing research has not yet solved this issue well enough to achieve a better conversion of qualitative and quantitative information. These problems result in the inability to provide effective guidance on actual construction.

A cloud model was proposed by D. Li in China. It mainly reflects the uncertainty in the concept of natural language, that is, fuzziness and randomness. Through the cloud generator, the cloud model can realize the transformation of qualitative and quantitative indicators and can effectively express the fuzzy uncertainty and random uncertainty of the concept [8].

Aiming at the deficiency of the existing evaluation models for the disaster risk of superlong tunnels, this study identifies the main disasters of deep-buried and superlong tunnels based on the cloud model. It considers four types of disasters and establishes a disaster risk evaluation system for highway tunnels. Based on the cloud droplet diagram, the fuzzy membership of the evaluation indicators is directly reflected to determine the risk level. Combined with a tunnel of the Chizhou-Qimen expressway, different sections of the tunnel are selected for evaluation, so as to evaluate the disaster risk and possibilities of the tunnel and provide reference for construction.

2. Materials and Methods

2.1. Risk Assess Methods. Figure 1 shows the basic framework and technical roadmap of the disaster risk evaluation system for superlong highway tunnels based on the cloud and AHP model. Its critical content includes the evaluation index system, evaluation criteria, the theory of the cloud model, numerical characteristics, verification, and conclusions. [1, 9, 10].

In this model, first, the AHP is used to calculate the index weight, and then, the numerical characteristics of the index are calculated by combining the cloud generator and the weight value. Finally, the membership degree is calculated to obtain the risk level of hazard sources in the tunnel.

2.2. Evaluation Index System. The superlong highway tunnel project traverses a wide area with complex geological conditions, diverse spatial forms, and high crustal stress. It is possible to occur some engineering geological hazards, such as hard rock bursts, soft surrounding rock deformations, collapses, water gushing and mud bursting, and high-temperature geothermal. Therefore, based on the reference of Chinese tunnel specifications, combined with some engineering practice experience [11–19], we establish the disaster risk evaluation index system of superlong highway tunnels. The system follows the principles of systematic, dynamic, and qualitative-quantitative combination and selects four kinds of geological hazards, such as water gushing and mud bursting, large rock deformation, rock burst, and collapse as the first-level indicators after fully considering the index factors affecting the occurrence of disasters from all aspects.

In Figure 2, water gushing and mud bursting are considered from three aspects: hydrogeological conditions, design and construction factors, and dynamic risk feedback. The degree of karst development (C1) and unfavorable geology (C2) is important for water gushing and mud bursting. The surrounding rock condition (C3) is the material basis of the development of the karst. The characteristics of the karst water system (C4) provide supplementary water for the development of the karst. The tunnel design (C5) ensures reasonable tunnel excavation. The excavation support structure (C6) ensures the stability of the surrounding rock. Tunnel construction disturbance (C7) affects the stability of the tunnel envelope.

The large rock deformation is considered from four aspects: hydrogeological conditions, ground stress conditions, design and construction factors, and dynamic risk feedback. High ground stress (B5) is the basic condition for large rock deformation generation. The formation lithology (C12) reflects the uniaxial compressive strength of the rock. The surrounding rock condition (C13) reflects the degree of fragmentation of the surrounding rock. Groundwater (C14) will have a softening effect on the rock. The excavation support structure (C15) ensures the stability of surrounding rock. The shape of the tunnel section (C16) affects the pressure on the supporting structure. The reserve deformation (C17) can ensure that the surrounding rock will not invade the secondary lining after deformation.

Rock burst is considered from four aspects: hydrogeological conditions, ground stress conditions, design and construction factors, and dynamic risk feedback. Under high ground stress conditions (B9), the stress in the rock mass is more concentrated and a rock burst is more likely to occur. The characteristics of groundwater (C22) affect the release of ground stress. The RQD index (C23) reflects the strength of the rock mass and the degree of rock fragmentation. The maximum storage strain energy of the rock mass (C24) is the limit of the occurrence of a rock burst. The length of single

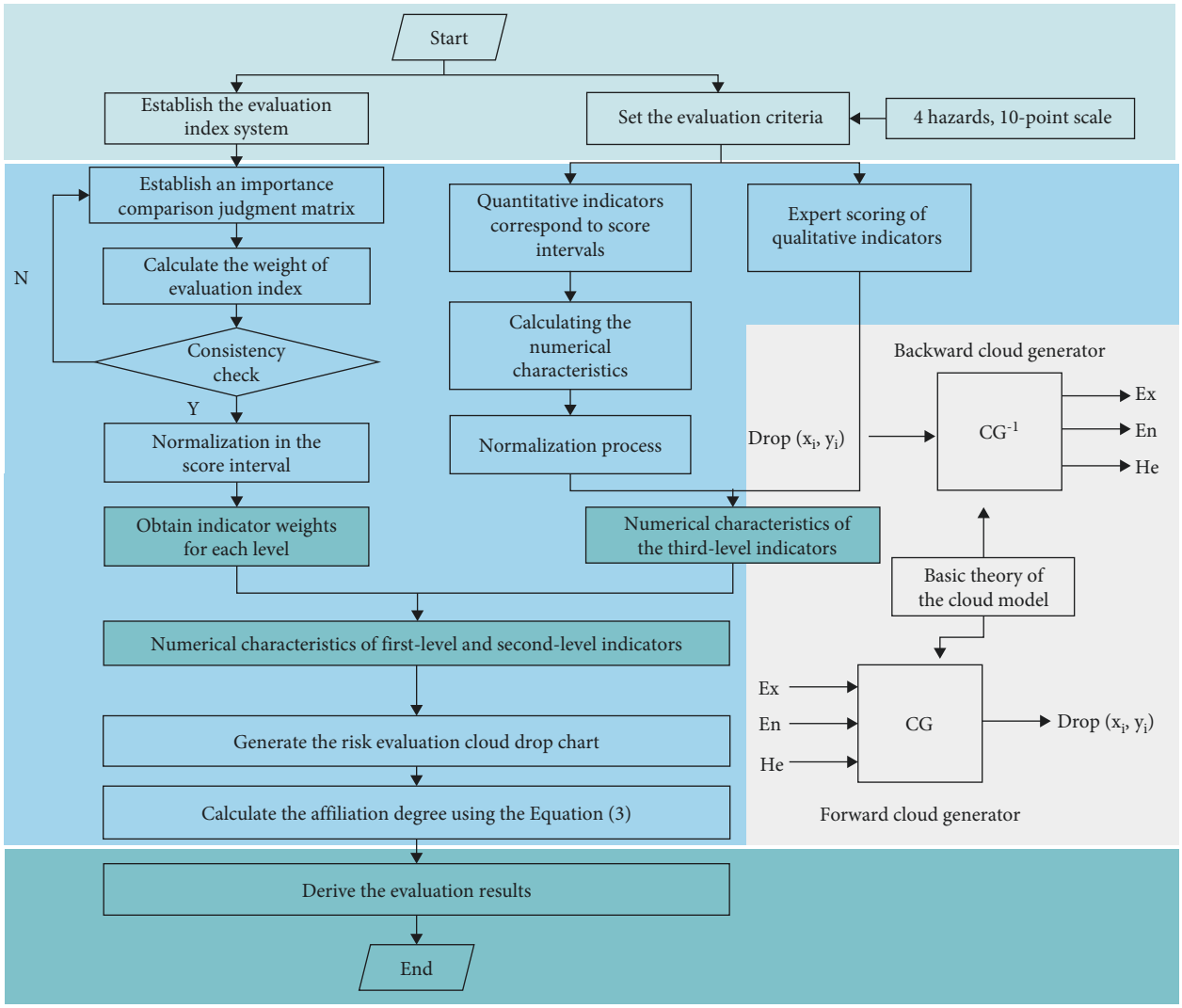

Figure 1: Flowchart of the evaluation model construction.

excavation (C25) affects the rock burst probability. A reasonable support structure (C26) ensures the stability of the tunnel. The depth of tunnel burial (C27) affects the magnitude of ground stress.

Collapse is considered from three aspects: hydrogeological conditions, design and construction factors, and dynamic risk feedback. The surrounding rock condition (C32) reflects the stability of the surrounding rock. The softening and dissolution of groundwater (C33) will aggravate the instability and collapse of rock mass. Unfavorable geology (C34) can lead to a potential release of stress and surrounding rock instability. The depth of tunnel burial (C35) and section size (C36) affect the stress of the surrounding rock. Advance support and lining (C37) ensure the stability of the surrounding rock.

Using the analytic hierarchy process (AHP) method, the evaluation indexes of each level of disaster risk in this evaluation system are scored by experts. The risk evaluation judgment matrix was derived based on the scoring results. After the consistency test and normalization process, the weight values of evaluation indicators at all levels were finally obtained, as shown in Table 1.

2.3. Basic Theories. In Figure 2, the establishment of the evaluation index system follows the principle of combining qualitative and quantitative values. In the subsequent evaluation process, it is inevitable to transform qualitative and quantitative. The cloud model, as an uncertainty model of qualitative and quantitative transformation, can fully reflect the randomness and fuzziness of evaluation indicators, which is an effective tool to realize accurate evaluation.

2.3.1. Cloud Model and Numerical Characteristics. Let U be a quantitative domain expressed by exact numerical values, and let C be a qualitative concept on U. If the quantitative value x is a random realization of the qualitative concept C, the certainty of x to C is $\mu(x) \in [0, 1]$ and $\mu(x)$ is a random number with a stable tendency. Then, the distribution on the

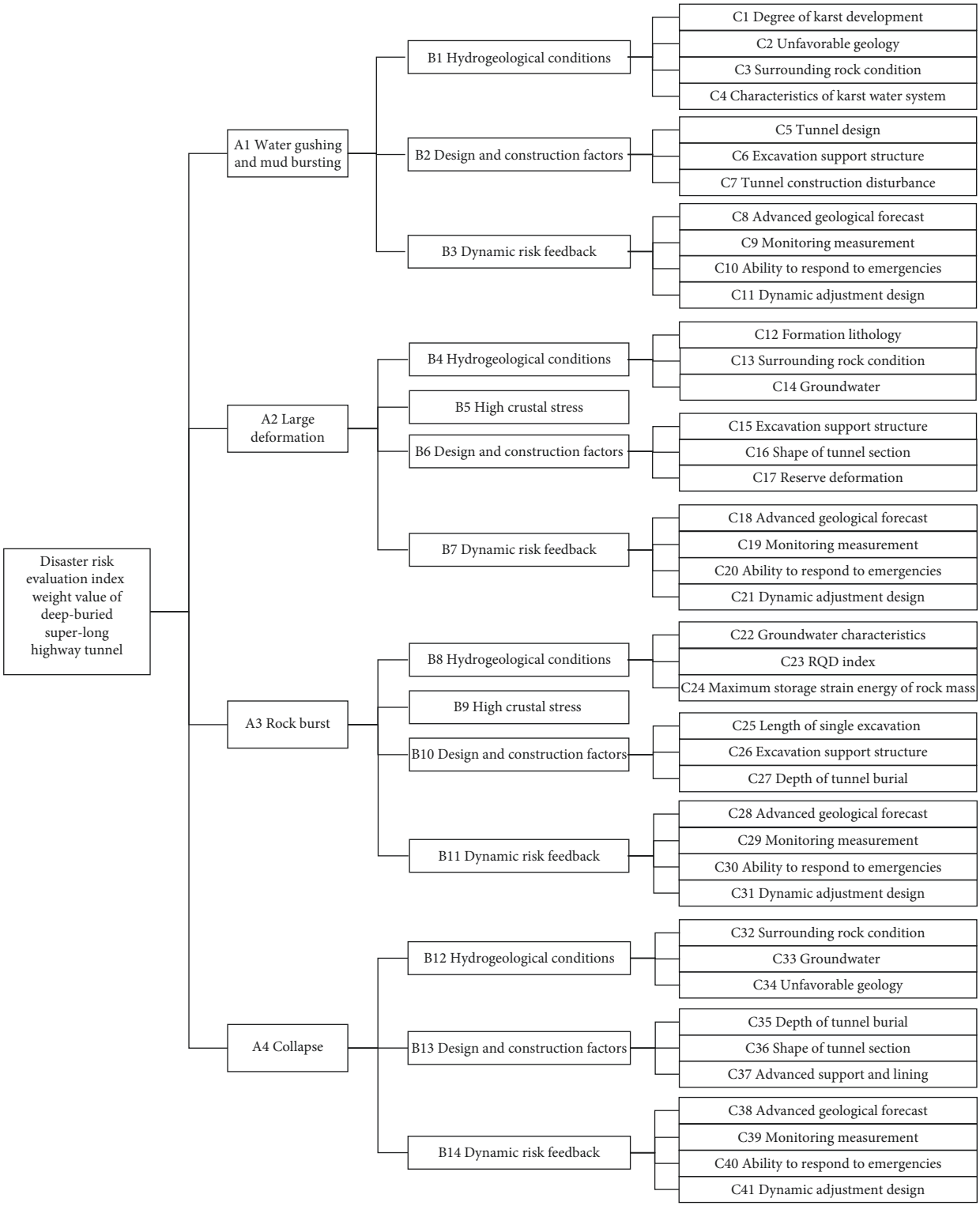

Figure 2: Disaster risk evaluation index of deep-buried and superlong highway tunnels.

universe U is called a cloud, and each x is called a cloud droplet.

$$\mu: U \longrightarrow [0,1], \quad \forall x \in U,\ x \longrightarrow \mu(x). \tag{1}$$

The numerical characteristics of the cloud are represented by expectation (Ex), entropy (En), and hyper entropy (He). Ex represents the expectation of cloud droplets' spatial distribution in the universe, which can represent the point of

Table 1: Evaluation index weight value.

First-level indicators	Weights	Second-level indicators	Weights	Third-level indicators	Weights
A_1	0.4065	B_1	0.6250	C_1	0.4181
				C_2	0.2226
				C_3	0.2497
				C_4	0.1096
		B_2	0.2385	C_5	0.5396
				C_6	0.2970
				C_7	0.1634
				C_8	0.2561
		B_3	0.1365	C_9	0.1380
				C_{10}	0.4778
				C_{11}	0.1281
A_2	0.1605	B_4	0.3370	C_{12}	0.5499
				C_{13}	0.2402
				C_{14}	0.2098
		B_5	0.4018		
		B_6	0.1640	C_{15}	0.5396
				C_{16}	0.1634
				C_{17}	0.2970
				C_{18}	0.2561
		B_7	0.0972	C_{19}	0.1380
				C_{20}	0.4778
				C_{21}	0.1281
A_3	0.0952	B_8	0.3370	C_{22}	0.2184
				C_{23}	0.6301
				C_{24}	0.1515
		B_9	0.4018		
		B_{10}	0.1640	C_{25}	0.1634
				C_{26}	0.2970
				C_{27}	0.5396
				C_{28}	0.2561
		B_{11}	0.0972	C_{29}	0.1380
				C_{30}	0.4778
				C_{31}	0.1281
A_4	0.3378	B_{12}	0.6250	C_{32}	0.3874
				C_{33}	0.4434
				C_{34}	0.1692
		B_{13}	0.2385	C_{35}	0.5278
				C_{36}	0.3325
				C_{37}	0.1396
		B_{14}	0.1365	C_{38}	0.2561
				C_{39}	0.1380
				C_{40}	0.4778
				C_{41}	0.1281

qualitative concept, or the most typical sample of quantitative concept. *En* is used to indicate the fuzziness of the numerical range. The numerical characteristics of *He* reflect the dispersion of cloud droplets.

When indicators have bilateral boundaries, such as $\in [a, b]$, the numerical characteristics are calculated as follows.

$$\begin{cases} E_x = \dfrac{(a+b)}{2}, \\ E_n = \dfrac{(b-a)}{6}, \\ H_e = i, \end{cases} \tag{2}$$

where i is the cloud droplet size control constant. It can be adjusted according to the uncertainty of specific cases and the fuzzy threshold of the index, which is 0.1 in this paper.

When the indicators have unilateral bounds, such as the intervals of the four evaluation levels of the evaluation factor x are I $(0, a)$, II (a, b), III (b, c), and IV $(c, +\infty)$, the numerical characteristics are calculated by the equations in Table 2.

2.3.2. Cloud Generator. A cloud generator is used to realize the conversion of qualitative and quantitative indicators. It is divided into the forward cloud generator (CG) and backward cloud generator (CG^{-1}). The forward cloud generator can realize the conversion from qualitative to quantitative,

Table 2: Rules for calculating numerical features of cloud models.

Risk level	Ex	En	He
I	$Ex_1 = (0 + a)/2$	$En_1 = (a - 0)/6$	0.1
II.	$Ex_2 = (a + b)/2$	$En_2 = (b - a)/6$	0.1
III	$Ex_3 = (b + c)/2$	$En_3 = (c - b)/6$	0.1
IV	$Ex_4 = c$	$En_4 = En_3$	0.1

and the backward cloud generator realizes the conversion from quantitative to qualitative as shown in Figure 3.

Based on MATLAB software, the numerical features of the cloud model can be presented in the form of cloud droplets. If the cloud droplet x satisfies $x \sim (Ex, En'^2)$, where $En'^2 \sim N(Ex, En^2)$, the certainty of x to qualitative concept can be obtained by formula (3).

$$\mu(x) = \exp\left[-\frac{(x - Ex)^2}{2(En')^2}\right], \tag{3}$$

where En' is a normal random number generated with En as the expected value and He is the standard deviation.

2.4. Evaluation Criteria. According to Chinese Railway Tunnel Risk Evaluation and Management Regulations and other related literature, the disaster risk status of superlong highway tunnels is classified into four levels: low risk, moderate risk, high risk, and extreme risk. We use the ten-point system to divide the four risk levels into sections, which are low risk (7.5 to 10), moderate risk (5 to 7.5), high risk (2.5 to 5), and extreme risk (0 to 2.5). According to equation (2), each risk level is converted into a standard comment cloud model, and the digital features are low risk (8.75, 0.42, 0.1), moderate risk (6.25, 0.42, 0.1), high risk (3.75, 0.42, 0.1), and extreme risk (1.25, 0.42, 0.1). The quantitative indicators are interval standardized and their risk factor levels are classified as shown in Table 3.

2.5. Evaluation Model. In the evaluation system, the qualitative risk index refers to expert scores and then uses the backward cloud generator to realize the transformation from the qualitative expert score to the cloud numerical characteristics parameter. Assuming that the subjective scores of n experts on an index are $P1, P2, \ldots, Pn$, respectively, the digital characteristics of the cloud model of the qualitative risk index can be obtained from (4).

$$\begin{cases} Ex_i = \dfrac{1}{n}\displaystyle\sum_{k=1}^{n} P_k, \\ En_i = \sqrt{\dfrac{\pi}{2}} \cdot \dfrac{1}{n}\displaystyle\sum_{k=1}^{n} \left|P_k - Ex_i\right|, \\ He_i = \sqrt{\dfrac{1}{n-1}\displaystyle\sum_{k=1}^{n} (P_k - Ex_i)^2 - En_i^2}, \end{cases} \tag{4}$$

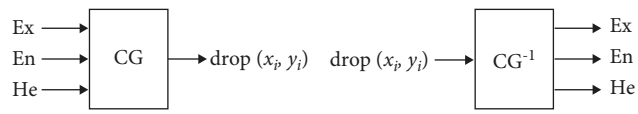

Figure 3: Forward and backward cloud generator.

where n is the number of experts and P_k is the score given by the k th expert.

The value of each quantitative indicator can be corresponded to the risk level in Table 2. If the value x lies within the risk level interval (m, n), the corresponding risk level interval is (a, b); then, according to (5), we can obtain the numerical characteristics of the quantitative index after normalization in the score interval.

$$\begin{cases} Ex_i = a + \dfrac{b - a}{n - m}(x - m), \\ En_i = \dfrac{(b - a)}{6}, \\ He_i = 0.1. \end{cases} \tag{5}$$

In order to reduce the deviation caused by the subjective tendency of the expert scoring method to the evaluation results, the numerical characteristics of the indicators should be combined with the weight value. Using (6), the numerical characteristics of the high-level indicators can be obtained by combining the numerical characteristics of the low-level indicators with the weight values.

$$\begin{cases} Ex = \dfrac{\sum_{i=1}^{m} Ex_i En_i \omega_i}{\sum_{i=1}^{m} En_i \omega_i}, \\ En = \displaystyle\sum_{i=1}^{m} En_i \omega_i, \\ He = \dfrac{\sum_{i=1}^{m} He_i En_i \omega_i}{\sum_{i=1}^{m} En_i \omega_i}, \end{cases} \tag{6}$$

where m is the number of low-level risk indicators subordinate to each high-level risk indicator, and ω_i is the weight value of each low-level risk indicator.

Using the forward cloud generator, the cloud droplet diagram for risk evaluation of each disasters can be generated. Then, to verify the accuracy of the evaluation results, we calculate the membership degree of each type of hazard to each risk level by (3). According to the cloud droplet

Table 3: Classification of a quantitative risk indicator.

Number	Quantitative indicator	Classification			
		Low risk	Moderate risk	High risk	Extreme risk
C16 C36	Shape of tunnel section/m^2	0~<10	10~<50	50~<100	≥100
C17	Reserved deformation/mm	≥120	80~<120	50~<80	30~<50
C25	Length of single excavation/m	0~<1	1~<2	2~<3	≥3
C27	Depth of tunnel burial/m	0~<50	50~<500	500~<1000	≥1000
C35	Depth of tunnel burial/m	≥500	100~<500	20~<100	0~<20

diagram and membership degree, we can determine the disaster risk level.

3. Case Study

3.1. Project Summary. A tunnel of the Chizhou-Qimen expressway has a total length of 4326 m. The tunnel mainly passes through strongly and moderately weathered sandstone and metamorphic sandstone. There are six fault zones in the tunnel, with the maximum buried depth of 740 m, which are located in the high crustal stress area. Four typical sections of the tunnel are selected for risk evaluation. The geological conditions of each section are described as follows:

The ZK69 + 491~ZK70 + 030 section is located in the high crustal stress area, crossing the metamorphic sandstone of medium weather. The lithology of the medium weather layer is hard and the tunnel excavation process is prone to produce rock bursts. This section is class IV surrounding rock, which is excavated by the drilling and blasting method, and the excavation method is an upper and lower bench method.

The ZK70 + 030~ZK70 + 355 section is located in the high crustal stress area and crosses the moderately weathered metamorphic sandstone. The lithology is soft and easy to produce large deformation of soft rocks during tunnel excavation. This section is class V surrounding rock, which is excavated by the drilling and blasting method, and the excavation method is an upper and lower bench method.

The ZK70 + 875~ZK71 + 005 section (buried depth of 40 ~ 74 m) of the right line of the tunnel is low (see Figure 4), and rainwater is easy to accumulate on the fault area. In this case, engineering geological problems such as water inrush and mud inrush may occur frequently during construction in rainy season. This section is class V surrounding rock, which is excavated by the drilling and blasting method, and the excavation method is an upper and lower bench method.

The tunnel portal section (ZK71 + 175~ZK71 + 360) mainly passes through the full-strength moderately weathered metamorphic sandstone. Joints and fractures are developed in the rock mass (see Figure 4). The section has shallow buried depth, bias pressure, and poor stability. Therefore, the tunnel is prone to collapse, sidewall instability, and even roof fall during construction. This section is class V surrounding rock, and the drilling and blasting method and the mechanical collaborative excavation method are adopted. The tunnel shall be supported in advance, and then excavated by steps.

In this paper, the abovementioned four tunnel sections are selected as key risk prevention and control sections for disaster risk evaluation of superlong highway tunnels, where the ZK70 + 875~ZK71 + 005 section is considered as rainy season construction.

3.2. Calculation of Numerical Characteristic. According to the measurement data and the engineering ground investigation report, the quantitative risk factor values are obtained in Table 4. The risk degree of each indicator is determined according to the risk classification table (see Table 3). Then, we can calculate the numerical characteristics of each indicator by (5).

The numerical characteristics of each indicator are calculated by the collective scores of experts and (4). Then, according to the weight values in Table 1, the numerical characteristics of the upper-level indicators are calculated by (6), and the first-level indicators of each sections are shown in Tables 5, 6, 7, and 8.

3.3. Results and Discussion. Taking section ZK69 + 491~ZK70 + 030 as an example, the evaluation cloud droplet diagram of this section is calculated with MATLAB software as shown in Figure 5.

In Figure 5, in section ZK69 + 491~ZK70 + 030, the cloud droplets of water gushing and mud bursting and collapse are nearby the grade of moderate risk, the cloud droplets of large deformation and rock burst are between moderate and high risk.

According to (3), the degree of membership degree of each risk level of the ZK69 + 491~ZK70 + 030 section can be calculated. The membership degrees of the four risk levels of large deformation are 0, 0.3399, 0.0028, and 0, respectively, and the membership degree of the medium level risk is the highest. The membership degrees of the four risk levels of rock burst are 0, 0.0187, 0.1172, and 0, respectively, and the membership degree of high risk is the highest. The results are consistent with the integrated evaluation cloud droplet diagram display. It can be inferred that the risk level of rock burst in this section is high risk.

Similarly, it can be deduced that the risk level of large deformation in section ZK70 + 030~ZK70 + 355 is high risk, and the risk level of other sections is of a moderate degree. The risk level of collapse in section ZK70 + 875~ZK71 + 005 and section ZK71 + 175~ZK71 + 360 is high risk, and the risk level of other sections is moderate.

The risk levels of each section are shown in Table 9.

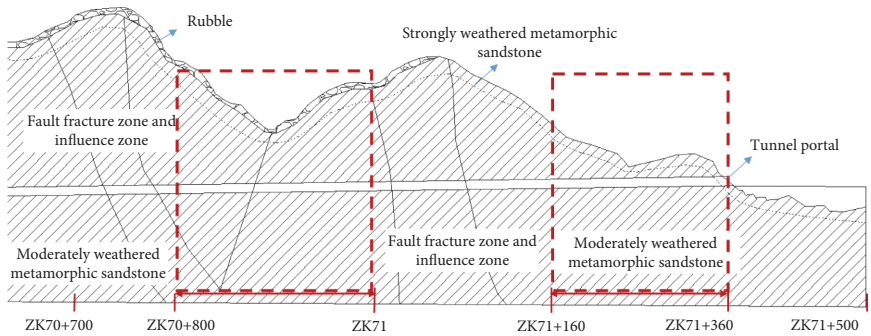

Figure 4: Geological profile of ZK70 + 700-ZK71 + 500 section.

Table 4: Values of quantitative risk factors.

Stake number	Shape of the tunnel section/ m^2	Reserved deformation/ mm	Length of single excavation/ m	Average buried depth/ m
ZK69 + 491~ZK70 + 030	77.86	80	1.5	570
ZK70 + 030~ZK70 + 355	77.86	100	0.7	366
ZK70 + 875~ZK71 + 005	77.86	100	0.7	61
ZK71 + 175~ZK71 + 360	77.86	150	0.5	23

Table 5: First-level indicators of section ZK69 + 491~ZK70 + 030.

Indicators	*Ex*	*En*	*He*
A_1	6.45	0.75	0.19
A_2	5.15	0.74	0.18
A_3	4.70	0.70	0.20
A_4	6.17	0.67	0.17

Table 6: First-level indicators of section ZK70 + 875~ZK71 + 005.

Indicators	*Ex*	*En*	*He*
A_1	6.42	0.69	0.30
A_2	4.97	0.62	0.25
A_3	5.19	0.58	0.26
A_4	5.88	0.59	0.28

Table 7: First-level indicators of section ZK70 + 875~ZK71 + 005.

Indicators	*Ex*	*En*	*He*
A_1	5.04	0.66	0.24
A_2	6.24	0.54	0.23
A_3	6.52	0.61	0.19
A_4	4.71	0.60	0.19

Table 8: First-level indicators of section ZK71 + 175~ZK71 + 360.

Indicators	*Ex*	*En*	*He*
A_1	5.66	0.63	0.28
A_2	6.48	0.63	0.27
A_3	6.79	0.59	0.28
A_4	4.72	0.62	0.23

In summary, the occurrence of rock burst and large deformation in high crustal stress section are usually frequent in tunnels. At the same time, the risks of collapse in the fault fracture zone and the cavern entrance section are also high. In the excavation process, there should be a targeted strengthening of these geological conditions in

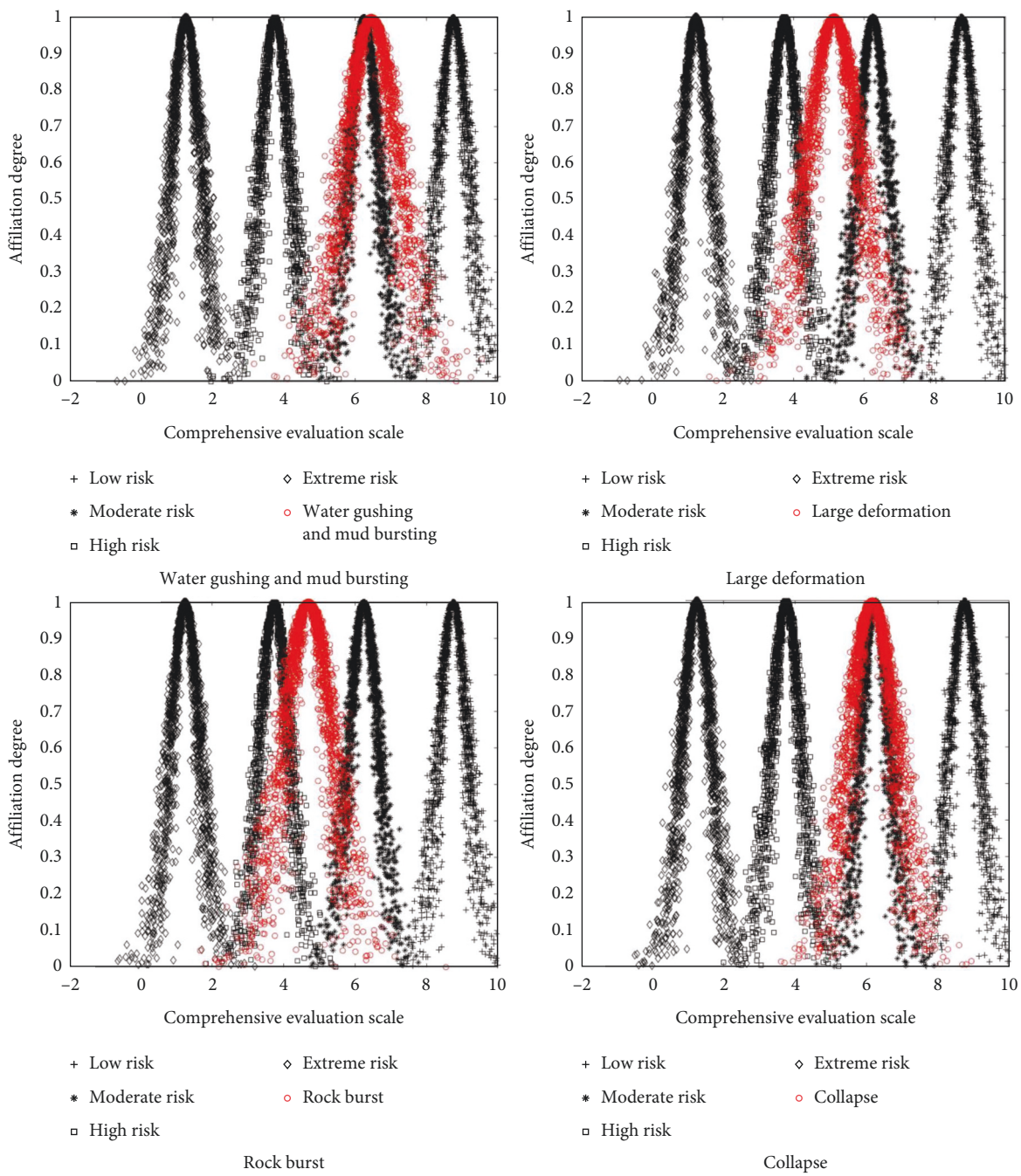

Figure 5: Cloud droplet diagram.

Table 9: Risk levels of each section.

Position	Water gushing and mud bursting	Large rock deformation	Rock burst	Collapse
ZK69 + 491~ZK70 + 030	Moderate risk	Moderate risk	High risk	Moderate risk
ZK70 + 030~ZK70 + 355	Moderate risk	High risk	Moderate risk	Moderate risk
ZK70 + 875~ZK71 + 005	Moderate risk	Moderate risk	Moderate risk	High risk
ZK71 + 175~ZK71 + 360	Moderate risk	Moderate risk	Moderate risk	High risk

advance geological forecasting, monitoring, and measuring work.

4. Conclusions

In this study, we use the cloud model theory and rely on a tunnel of the Chizhou-Qimen expressway to study the disaster risk evaluation of the superlong tunnel and draw the following conclusions.

(1) Selecting water gushing and mud bursting, large rock deformation, rock burst, and collapse as the four possible geological disasters of superlong tunnels as the first-class indicators, a disaster risk evaluation model of superlong tunnels based on cloud model theory is established. The model comprehensively represents the possible geological disaster risk state in the tunnel construction stage.

(2) In superlong highway tunnel engineering, this paper selects four typical sections for evaluation. The results show that the hard rock part of the tunnel with high crustal stress has a higher risk of rock burst, the soft rock part has a higher risk of large deformation, and the fault section and the entrance section of the tunnel have a higher risk of collapse. This study can provide a reference for preventing the occurrence of superlong tunnel disasters as well as adopting effective excavation schemes and supporting measures.

(3) The cloud model cloud drop map generated by the forward cloud generator can intuitively obtain the risk grade results of each disaster. Moreover, the corresponding digital features are used to calculate the membership degree to verify the results, which is more authentic and reliable.

(4) The cloud model-based disaster risk evaluation model for superlong highway tunnels realizes the transformation between multiperson decision assignment and engineering measured values. This evaluation model improves the objectivity of risk evaluation and provides a new way of thinking for disaster risk evaluation of deep-buried and superlong tunnels.

Data Availability

The data used to support the findings of this study are available from the corresponding author upon request.

Conflicts of Interest

The authors declare no conflicts of interest.

Acknowledgments

The authors thank Road and Bridge South China Engineering Co., Ltd. For their assistance with conducting the field experiments. The research has been supported by the Initiation fund for Postdoctoral Research of Central South University, grant no. 228697.

References

[1] T. Xu, Z. Song, D. Guo, and Y. Song, "A cloud model-based risk assessment methodology for tunneling-induced damage to existing tunnel," *Advances in Civil Engineering*, vol. 2020, Article ID 8898362, 11 pages, 2020.

[2] Q. Wang, S. Qiu, Y. Cheng, and X. Chen, "Method of evaluation of rockburst classification based on GIS for deeply-buried ultra-long tunnels," *Journal of Central South University*, vol. 52, pp. 2572–2587, 2021.

[3] R. Song, D. Zhang, and M. Wen, "The cusp catastrophe theory analysis for instability of deep-buried tunnels surrounding rock through fault fracture zone," *China Civil Engineering Journal*, vol. 48, pp. 289–292, 2015.

[4] X. Jia, "The prediction of rock burst, large deformation and their risk assessment for Erlang Mountain Tunnel Sichuan-Tibet railway," Chengdu University of Technology, Chengdu, China, Master's Degree, 2016.

[5] Z. Xu, S. Li, and L. Li, "Risk assessment of water or mud inrush of karst tunnel based on analytic hierarchy process," *Rock and Soil Mechanics*, vol. 32, pp. 1757–1766, 2011.

[6] B. Wu, W. Qiu, and G. Meng, "Evaluation of possibility of tunnel collapse base on fuzzy analytic network process," *Mathematics In Practice And Theory*, vol. 51, pp. 127–136, 2021.

[7] W. Guo, C. Yang, W. Bo et al., "Risk assessment of shield tunnel construction in karst strata based on fuzzy analytic hierarchy process and cloud model," *Shock and Vibration*, vol. 2021, Article ID 7237136, 16 pages, 2021.

[8] D. Li, H. Meng, and X. Shi, "Membership clouds and membership cloud generaors," *Computer R&D*, vol. 32, pp. 15–20, 1995.

[9] D. Liu, M. Cao, Y. Tang, and Q. Xu, "Risk evaluation of water inrush in water-rich karst tunnel based on cloud model," *Journal of Safety Science and Technology*, vol. 17, pp. 109–115, 2021.

[10] Y. Xia, Z. Xiong, Z. Wen, H. Lu, and X. Dong, "Entropy-based risk control of geological disasters in mountain tunnels under uncertain environments," *Entropy*, vol. 20, no. 7, p. 503, 2018.

[11] C. Zheng, B. Chen, W. Li, and Z. Zhang, "Research on risk assessment of complex mountain tunnels based on AHP-FCE," *IOP Conference Series: Materials Science and Engineering*, vol. 741, no. 1, Article ID 012031, 2020.

[12] X. Kuang, M. Bai, and C. Wang, "Study on risk assessment and control technology for safe construction of deep buried high geostress tunnel," *Subgrade Engineering*, vol. 27, pp. 100–103, 2010.

[13] C. Ma, J. Fan, X. Ji, X. Shi, and J. Zeng, "Effect of the initial support of the tunnel on the characteristics of rockburst: case study and mechanism analysis," *Advances in Civil Engineering*, vol. 2022, Article ID 7235619, 16 pages, 2022.

[14] H. Zhang, L. Chen, Y. Zhu, Z. Zhou, and S. Chen, "Stress field distribution and deformation law of large deformation tunnel excavation in soft rock mass," *Applied Sciences*, vol. 9, no. 5, p. 865, 2019.

[15] C. Caliendo, G. Genovese, and I. Russo, "Risk analysis of road tunnels: a computational fluid dynamic model for assessing the effects of natural ventilation," *Applied Sciences*, vol. 11, no. 32, 2021.

[16] L. Zhang and H. Li, "Construction risk assessment of deep foundation pit projects based on the projection pursuit method and improved set pair analysis," *Applied Sciences*, vol. 12, no. 1922, 2022.

[17] S. Qiao, Z. Cai, J. Tan, P. Xu, and Y. Zhang, "Analysis of collapse mechanism and treatment evaluation of a deeply buried hard rock tunnel," *Applied Sciences*, vol. 10, p. 4297, 2020.

[18] D. Wang, J. Luo, K. Shen, L. Gao, F. Li, and L. Wang, "Analysis of the causes of the collapse of a deep-buried large cross-section of loess tunnel and evaluation of treatment measures," *Applied Sciences*, vol. 12, no. 161, 2022.

[19] X. Wang, K. Shi, Q. Shi, H. Dong, and M. Chen, "A normal cloud model-based method for risk assessment of water inrush and its application in a super-long tunnel constructed by a tunnel boring machine in the arid area of northwest China," *Water*, vol. 12, no. 3, p. 644, 2020.